Statistical Bootstrap Model In The Partonic Phase

Alexander Gehwald

Dr. K. Gallmeister, Prof. Dr. C. Greiner

Johann Wolfgang Goethe-Universität Frankfurt am Main

March 21, 2023

Motivation

Fire-balls which consist of fire-balls, which consist of fire-balls, which...

(R. Hagedorn [4])

$$\tau(m) \sim m^a \exp\left(\frac{m}{T_H}\right) \tag{1}$$

$$N_{\mathrm{mass}}(m) = \int \mathrm{d}m\, \tau(m) \tag{2}$$

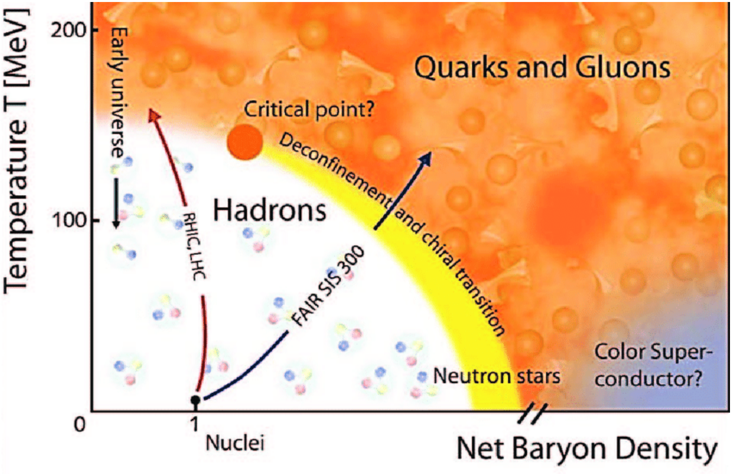

Figure 1: Illustration of QCD phase diagram (taken from [5])

Motivation

Hadronic Hagedorn States

- Transition from QGP to HRG in UrQMD by Beitel et al. [1, 2]
- Bootstrap with (B, S, I) instead of (B, S, Q) by Gallmeister et al. [3]

Question

Can we implement a similar framework with partonic particles?

Motivation

Outline

- Implement partonic bootstrap model and numerical framework
- Thermodynamics $\Rightarrow$ transport
  - Dynamic box simulation
  - Explicitly break detailed balance by removing white particles to simulate hadronization

Motivation

Hadronic $\rightarrow$ partonic

$(B, S, Q) \rightarrow (r, g, b, Q, q)$

- $u, \bar{u}, d, \bar{d}, g$
- Color charges r, g, b
- Electric charge Q
- Quark count q
- Hagedorn radius R, with $V = \frac{4}{3}\pi R^3$
- Particle masses m_q, m_g

Bootstrap

$$\tau_{\vec{Q}}(m) = \frac{V}{(2\pi)^2}\frac{1}{2m}\tilde{\sum}\iint \mathrm{d}m_1\mathrm{d}m_2\,\tau_{\vec{Q}_1}(m_1)\tau_{\vec{Q}_2}(m_2)\,m_1 m_2\,p_{cm}(m, m_1, m_2) \quad (3)$$

$$p_{cm}(m, m_1, m_2) = \frac{1}{2m}\sqrt{(m^2 - (m_1 - m_2)^2)\,(m^2 - (m_1 + m_2)^2)} \quad (4)$$

$$\tilde{\sum} \equiv \sum_{\vec{Q}_1, \vec{Q}_2} \delta^3_{\vec{Q}, \vec{Q}_1 + \vec{Q}_2} \quad (5)$$

$$\vec{Q} \equiv (r, g, b, Q, q) \quad (6)$$

$$\tau_{\vec{Q}}(m) = \frac{g_\alpha}{\Delta m}\delta(m - m_\alpha)\delta(\vec{Q} - \vec{Q}_\alpha) \;\;,\;\; \alpha \in [g, q, \bar{q}] \quad (7)$$

Bootstrap

$$\Gamma_{1\to 2}(m) = \frac{\sigma_{2\to 1}}{4\pi^2 \tau_{\vec{Q}}(m)} \tilde{\sum} \iint \mathrm{d}m_1 \tau_{\vec{Q}_1}(m_1) \mathrm{d}m_2 \tau_{\vec{Q}_2}(m_2) p_{cm}^2(m, m_1, m_2) \tag{8}$$

$$\sigma_{2\to 1} = \pi R^2 \tag{9}$$

Abelian Approximation

Problem

Three colours results in more loops which increases computation time heavily.

Solution

Abelian approximation [7] to take a $U(1) \times U(1)$ abelian subgroup of the full $SU(3)$ QCD group. Treat two commuting gluon fields as classical fields and then neglect them (but keep the other 6 gluons), allowing expression of colour charge as (λ_3, λ_8).

$$\Rightarrow \vec{Q} \equiv (\lambda_3, \lambda_8, Q, q) \tag{10}$$

Abelian Approximation

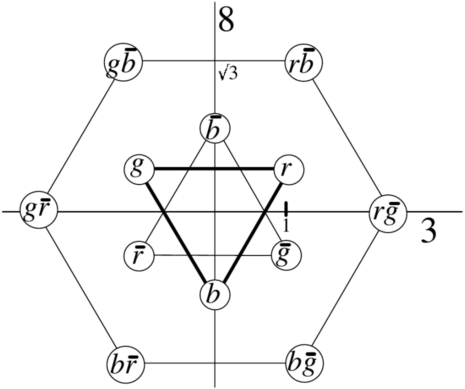

Figure 2: Quark and gluon colour charges in the abelian approximation. Figure taken from [7]

Bootstrap - Discretization

$$\tau_{\vec{Q}}(n) = \frac{V}{(2\pi)^2} \frac{(\Delta m)^4}{(2n)^2} \tilde{\sum} \sum_{j=i^0_{\vec{Q}_1}}^{n-1} \sum_{k=i^0_{\vec{Q}_2}}^{n-1-j} j \cdot k \cdot \tau_{\vec{Q}_1}(j) \tau_{\vec{Q}_2}(k) S_{njk} \tag{11}$$

$$\Gamma_{1\to 2,\vec{Q}}(n) = \frac{\sigma_{2\to 1}(\Delta m)^4}{(4n\pi)^2 \tau_{\vec{Q}}(n)} \tilde{\sum} \sum_{j=i^0_{\vec{Q}_1}}^{n-1} \sum_{k=i^0_{\vec{Q}_2}}^{n-1-j} \tau_{\vec{Q}_1}(j) \tau_{\vec{Q}_2}(k) S^2_{njk} \tag{12}$$

with

$$S_{ijk} = \sqrt{\left(i^2 - (j-k)^2\right)\left(i^2 - (j+k)^2\right)} \tag{13}$$

$$V = \frac{4}{3}\pi R^3 \tag{14}$$

Bootstrap - Discretization

$$N_\lambda := \text{maximum value of } \lambda_3 \text{ and } \lambda_8 : \qquad \lambda_3, \lambda_8 \in [-N_\lambda, N_\lambda] \tag{15}$$

$$N_Q := \text{maximum value of } Q : \qquad Q \in [-N_Q, N_Q] \tag{16}$$

$$N_q := \text{maximum value of } q : \qquad q \in [0, N_q] \tag{17}$$

Results

$R = 0.3\text{fm}, \Delta m = m_q = 0.1\,\text{GeV}, m_g = 0.3\,\text{GeV}, N_\lambda = 20, N_Q = N_q = 10$

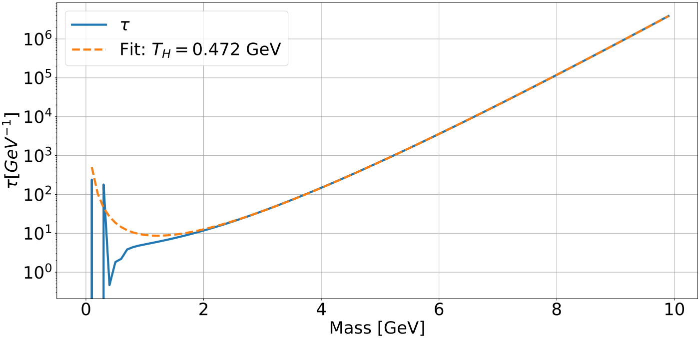

Figure 3: Example of Hagedorn spectrum and fit for T_H

Results - Quantum Number Limits

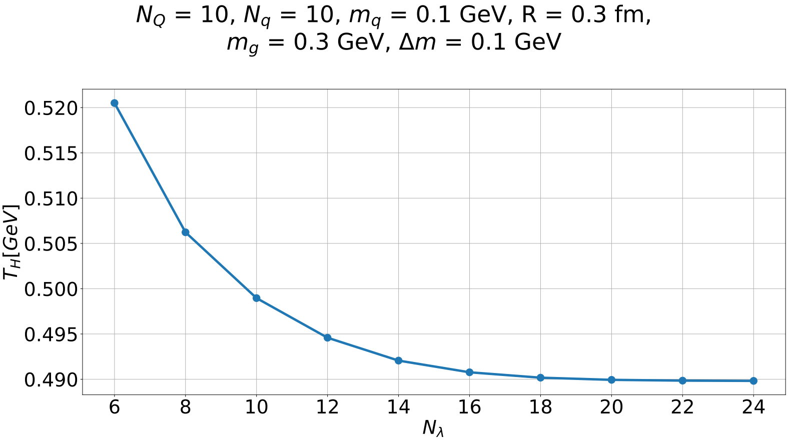

Figure 4: Effect of varying N_λ on T_H.

Results - Quantum Number Limits

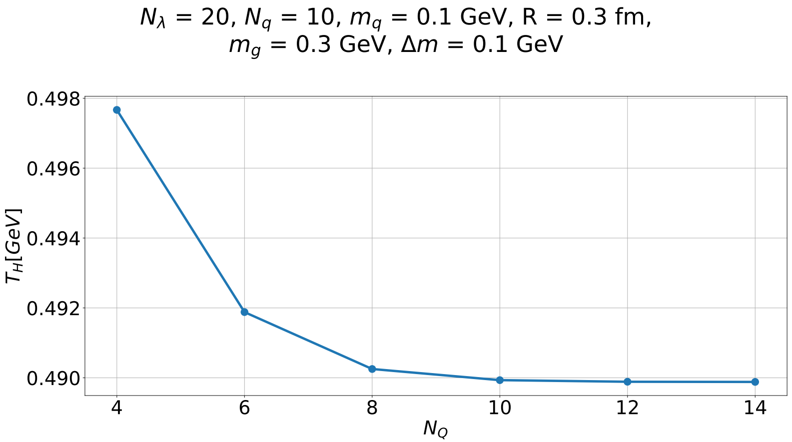

Figure 5: Effect of varying N_Q on T_H.

Results - Quantum Number Limits

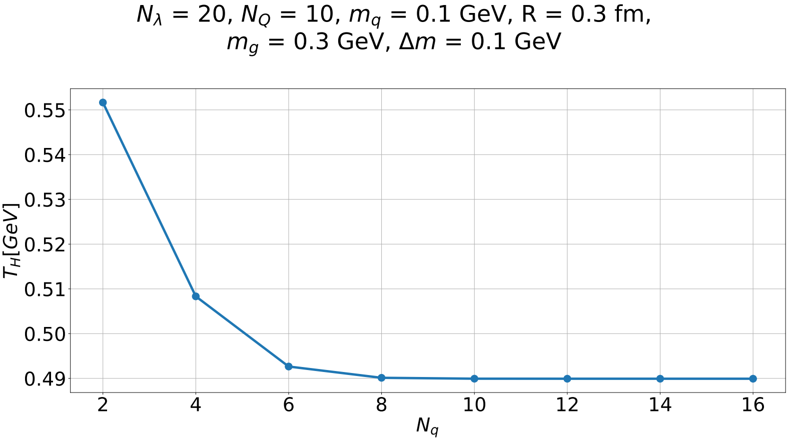

Figure 6: Effect of varying N_q on T_H.

Results - Radius

$\Delta m = m_q = 100\,\text{MeV}, m_g = 300\,\text{MeV}, N_\lambda = 20, N_Q = N_q = 10$

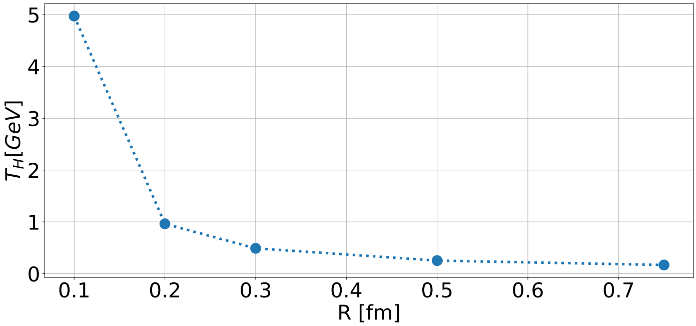

Figure 7: Dependency of T_H from Hagedorn radius R for a given set of other parameters. The connecting line is just to guide the eye.

Results - Bin Width

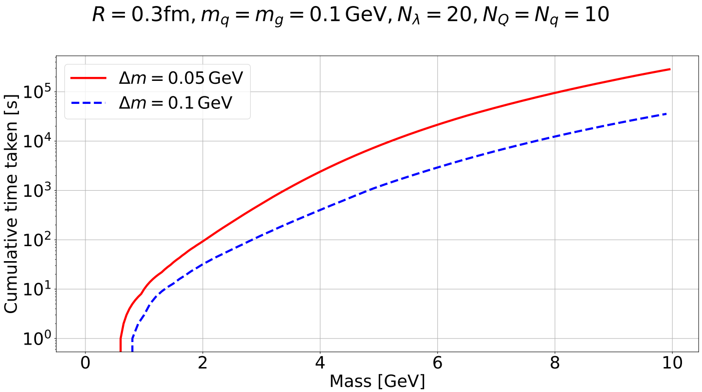

Figure 8: Examples of the influence of the number of mass bins on the runtime of the bootstrap process (Intel(R) Core(TM) i5-6500 CPU @ 3.20GHz).

Results - Bin Width

$R = 0.3\,\text{fm}, m_q = 0.1\,\text{GeV}, m_g = 0.1\,\text{GeV}, N_\lambda = 20, N_Q = N_q = 10$

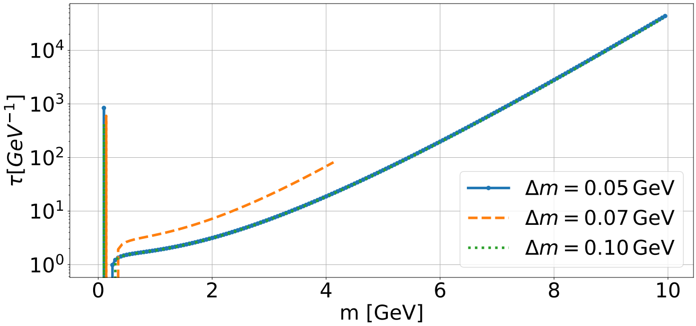

Figure 9: Comparison of Hagedorn spectrum for different values of Δm while keeping the other parameters constant.

Results - Decay Width

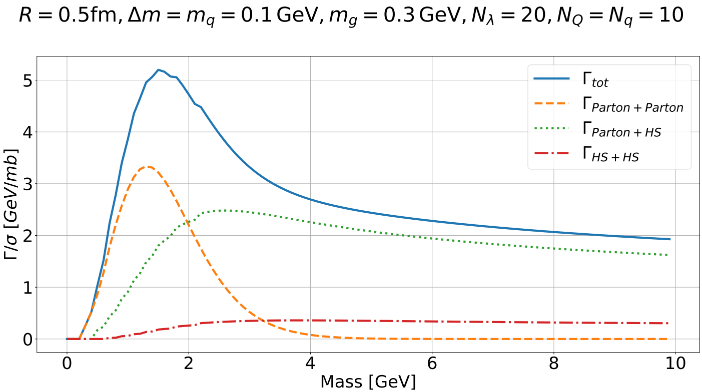

Figure 10: $\Gamma_{(0,0,0)}$ split up in the contributions of parton + parton, parton + Hagedorn state, and Hagedorn state + Hagedorn state interactions.

Box Simulations

- Checking detailed balance
- Explicitly violating detailed balance
- Obtaining the mass distribution of white particles

Common parameters: $V_{box} = 1000\,\mathrm{fm}^3$, $T_H \sim 250\,\mathrm{MeV}$, $T_{box} = 180\,\mathrm{MeV}$.

Box Simulations

$$2 \to 1 : \sigma_{2\to 1} = \pi R^2 \tag{18}$$

$$1 \to 2 : \Gamma_{1\to 2,\vec{Q}}(n) = \frac{\sigma_{2\to 1}(\Delta m)^4}{(4n\pi)^2 \tau_{\vec{Q}}(n)} \tilde{\sum} \sum_{j=i^0_{\vec{Q}_1}}^{n-1} \sum_{k=i^0_{\vec{Q}_2}}^{n-1-j} \tau_{\vec{Q}_1}(j)\tau_{\vec{Q}_2}(k) S^2_{njk} \tag{19}$$

Optional $2 \to 2$ with fixed cross section for momentum redistribution.

Box Simulations

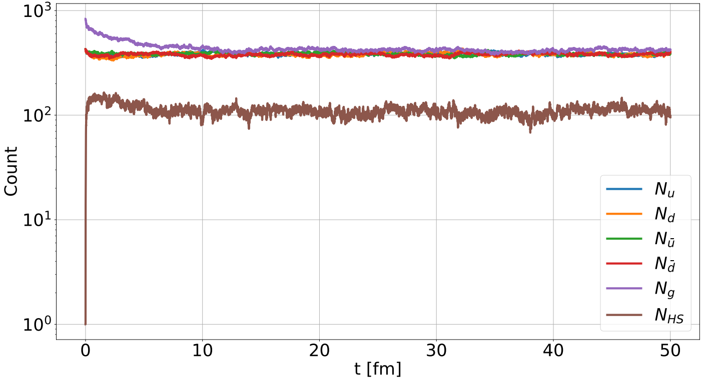

Figure 11: Time evolution of box contents by particle species for $T = 180\,\mathrm{MeV}$

Box Simulations

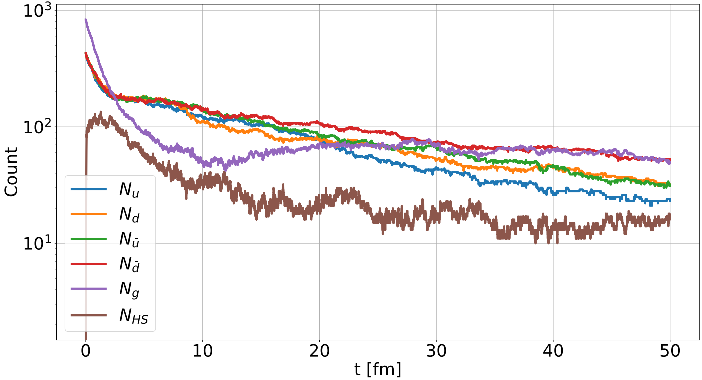

Figure 12: Time evolution of box contents by particle species for $T = 180\,\mathrm{MeV}$ without detailed balance

Box Simulations

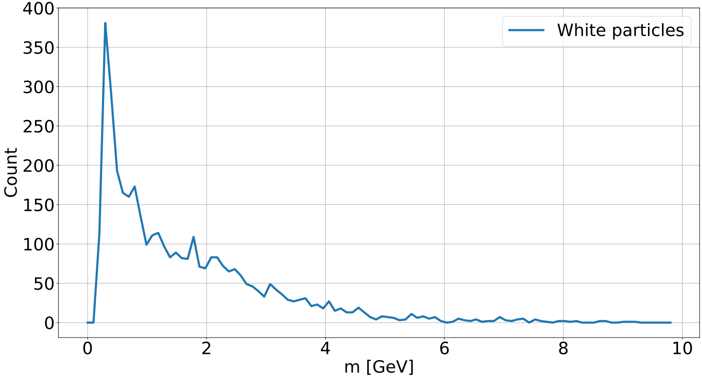

Figure 13: Mass distribution of white particles in box simulation for $T = 180\,\mathrm{MeV}$

Box Simulations

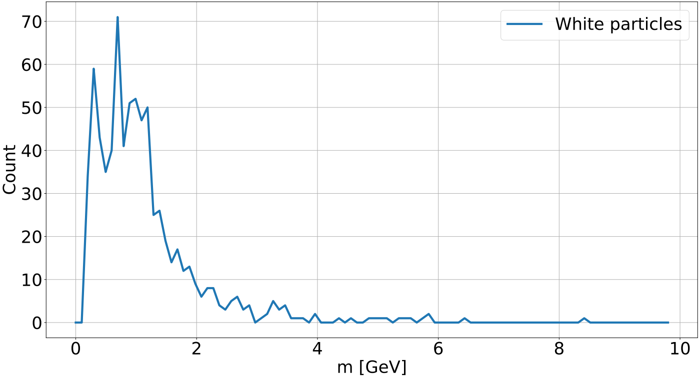

Figure 14: Mass distribution of white particles in box simulation for $T = 180\,\mathrm{MeV}$ without detailed balance

Conclusions and outlook

Summary

- We implemented a numerical framework for the partonic bootstrap
- Parameter choice matters
- Decay widths can get rather large
- Box simulations reach equilibrium fairly quickly
- Mass distribution of white particles

Outlook

Future studies can look deeper into the details and match white particles to hadronic Hagedorn states to further decay via hadronic channels.

References I

[1] M. Beitel. "Thermalization of Hadrons via Hagedorn States". PhD thesis. Johann Wolfgang Goethe-Universität Frankfurt am Main, 2016.

[2] M. Beitel, K. Gallmeister, and C. Greiner. "Equilibration of hadrons in HICs via Hagedorn States". In: *Journal of Physics: Conference Series* 668 (Jan. 2016). arXiv: 1509.01416, p. 012057. ISSN: 1742-6588, 1742-6596. DOI: 10.1088/1742-6596/668/1/012057. URL: http://arxiv.org/abs/1509.01416 (visited on 10/19/2021).

[3] K. Gallmeister and C. Greiner. "Production of light nuclei in heavy ion collisions via hagedorn resonances". In: *Eur. Phys. J. A* 57.2 (2021), p. 62. DOI: 10.1140/epja/s10050-020-00329-z. arXiv: 2007.08258 [hep-ph].

[4] R. Hagedorn. "Statistical thermodynamics of strong interactions at high-energies". In: *Nuovo Cim. Suppl.* 3 (1965), pp. 147–186.

[5] Johann M. Heuser. "The Compressed Baryonic Matter Experiment at FAIR: Progress with feasibility studies and detector developments". In: *Nucl. Phys. A* 830 (2009). Ed. by Paul Stankus et al., pp. 563C–566C. DOI: 10.1016/j.nuclphysa.2009.09.048. arXiv: 0907.2136 [nucl-ex].

References II

[6] John Maddock and Christopher Kormanyos. *Boost C++ Libraries*. Last accessed 01-02-2023. 2023. URL: https://www.boost.org/doc/libs/1_81_0/libs/multiprecision/doc/html/index.html.

[7] C. T. Traxler, U. Mosel, and T. S. Biró. "Hadronization of a quark-gluon plasma in the chromodielectric model". en. In: *Physical Review C* 59.3 (Mar. 1999), pp. 1620–1636. ISSN: 0556-2813, 1089-490X. DOI: 10.1103/PhysRevC.59.1620. URL: https://link.aps.org/doi/10.1103/PhysRevC.59.1620 (visited on 04/16/2021).

Appendix

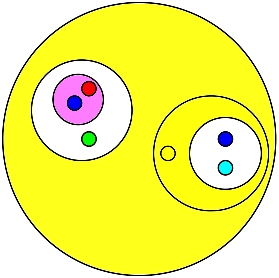

Figure 15: Example illustration of a coloured Hagedorn state. The coloured dots represent (anti-)quarks or gluons: the green, blue, and red dots represent green, blue, and red quarks respectively, the yellow one is an antired quark, and the turquoise one is an antiblue quark. This example results in the state consisting of the blue and antiblue quarks and the state made up from the green quark and the state consisting of a red and blue quark to be white, however due to the antired quark (yellow), the colour of the right tier 2 Hagedorn state as well as the final state is antired.

Appendix - Arbitrary Precision Calculations

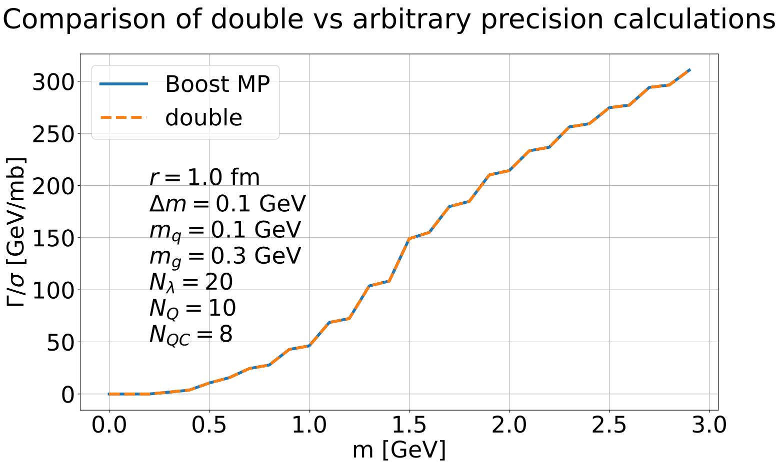

Figure 16: Comparison of $\frac{\Gamma(m)}{\sigma_{2\to1}}$ using the standard floating point datatype "double" versus the arbitrary precision data type of the Boost Multiprecision library [6].

Appendix - Emulating Pions

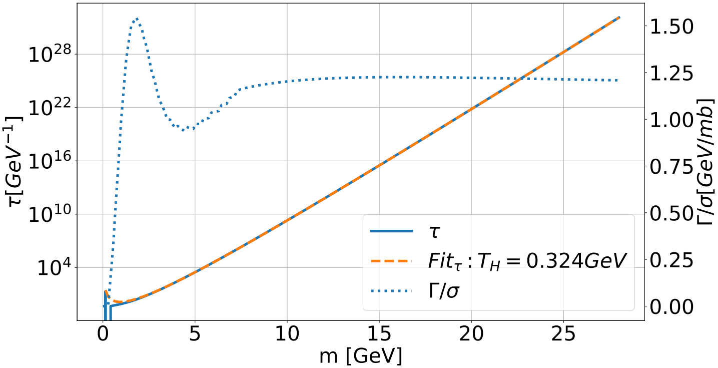

Figure 17: Bootstrap process using pions as initial conditions.

$R = 0.3\text{fm}, \Delta m = m_q = 0.1\,\text{GeV}, m_g = 0.3\,\text{GeV}, N_Q = N_q = 10$

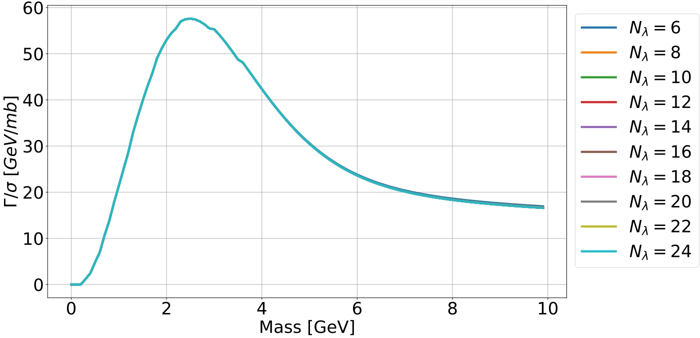

Figure 18: Influence of N_λ on $\Gamma_{(0,0,0)}$

Appendix - Influence on Gamma

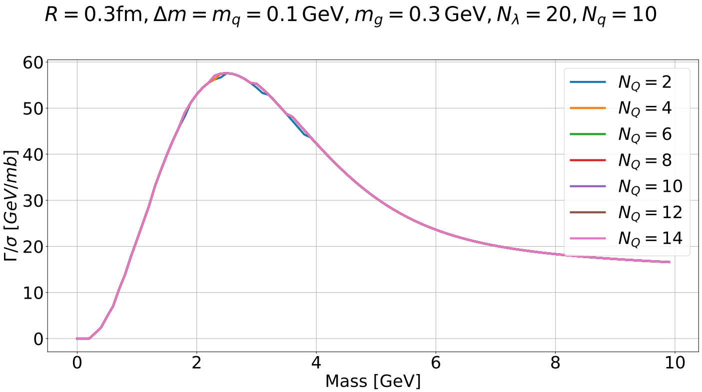

Figure 19: Influence of N_Q on $\Gamma_{(0,0,0)}$

Appendix - Influence on Gamma

$R = 0.3\text{fm}, \Delta m = m_q = 0.1\,\text{GeV}, m_g = 0.3\,\text{GeV}, N_\lambda = 20, N_Q = 10$

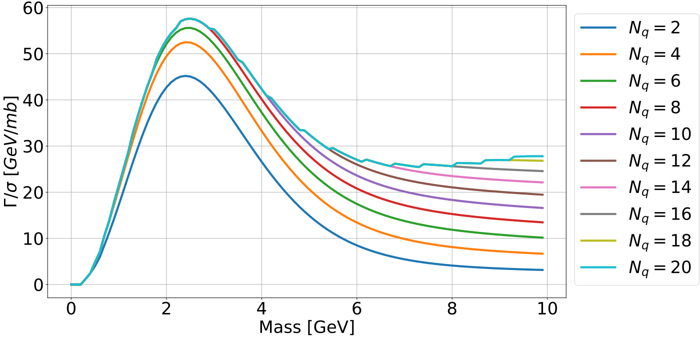

Figure 20: Influence of N_q on $\Gamma_{(0,0,0)}$